6-2003

Quarterly Report for the TRP Project, March–June 2003

Samir Moujaes
University of Nevada, Las Vegas, samir@me.unlv.edu

Yitung Chen
University of Nevada, Las Vegas, yitung.chen@unlv.edu

Kanthi Kiran Daiska
University of Nevada, Las Vegas

Chao Wu
University of Nevada, Las Vegas

Quarterly Report for the TRP Project at the
March–June 2003

Samir .F. Moujaes, Yitung Chen, Kanthi Kiran Dasika, Chao Wu

Overall Corrosion Modeling:

Closed Rectangular Loop Model:

The MTL is assumed to be a 5m long rectangular loop with a circular cross-section. Because of the non-symmetry, and due to the active participation of the secondary flows due to the elbows present in the rectangular loop model, the geometry is considered as a 3D model, as shown in the figure 1. As can be seen, the region near the wall has been greatly refined, because, the mass diffusion from the wall into the fluid is very prominent in near the wall region than in the bulk of the fluid. In order to capture these details, the region near the wall has been refined to a fair degree.

Figure 1: Closed rectangular loop model

Momentum source has been introduced in the model to account for the pump in the MTL. The model has been tested for both laminar and turbulent flow regimes the Reynolds' number being 2000 for the laminar flow and 200,000 for the turbulent flow. The velocity, temperature and concentration profiles at the elbow sections for each of these runs have been shown in the following figures. Figures 2 & 3 show the velocity profiles at the elbow section for the laminar ant turbulent regimes.

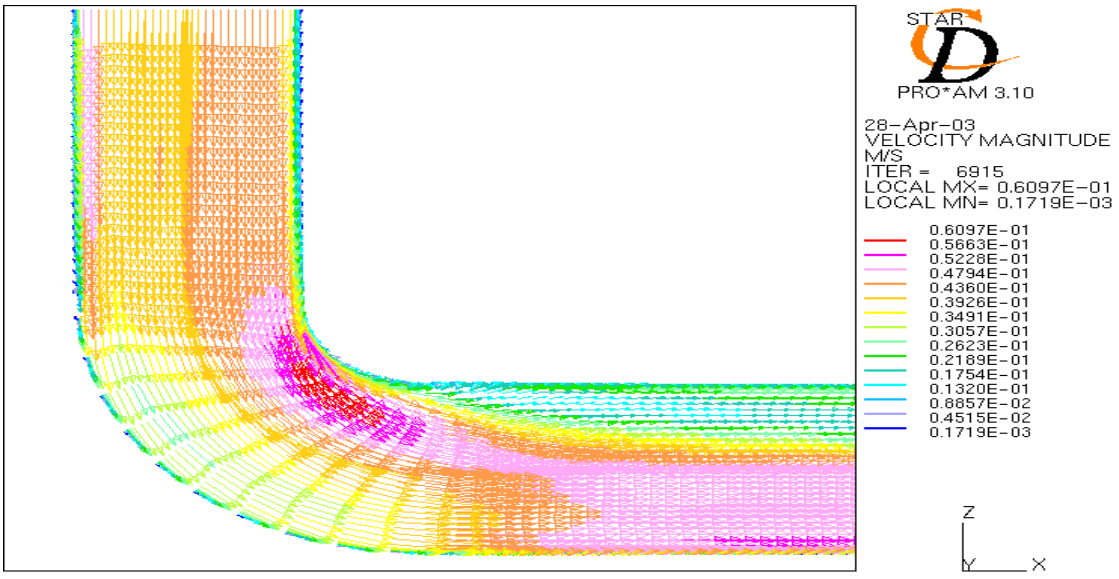

Figure 2: Velocity profile at an elbow section for the laminar flow in the rectangular loop model

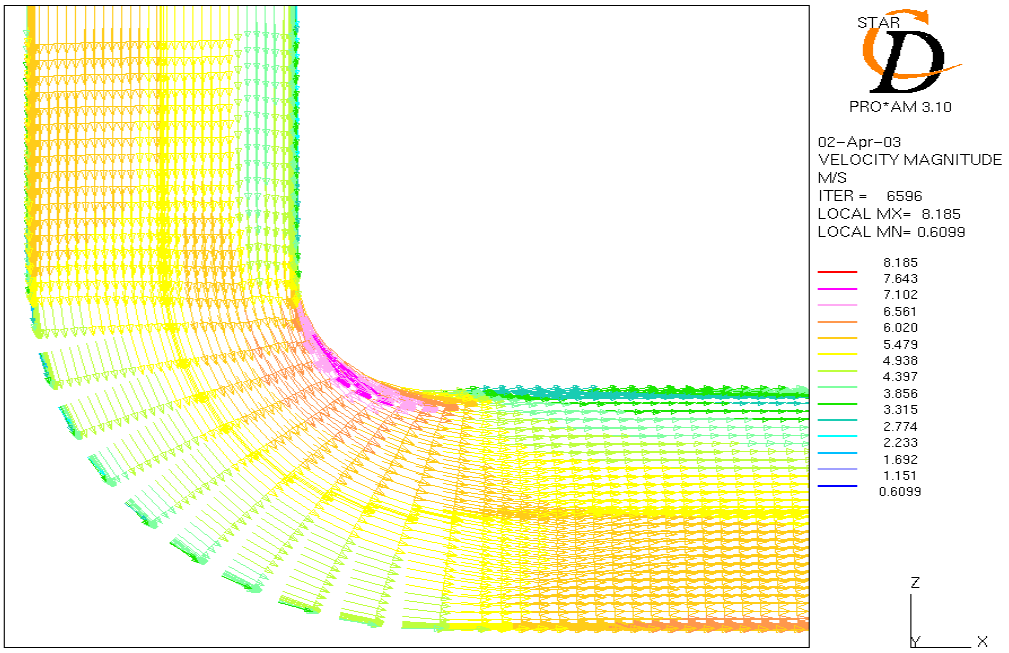

Figure 3: Velocity profile at an elbow section for the turbulent flow in the rectangular loop model

The temperature variation along the whole length of the loop for a laminar flow is shown in figure 4. The diffusion of temperature from the walls into the fluid is clearly seen all along the loop. Figure 5 shows the temperature distribution at an elbow section of the rectangular loop for a turbulent flow.

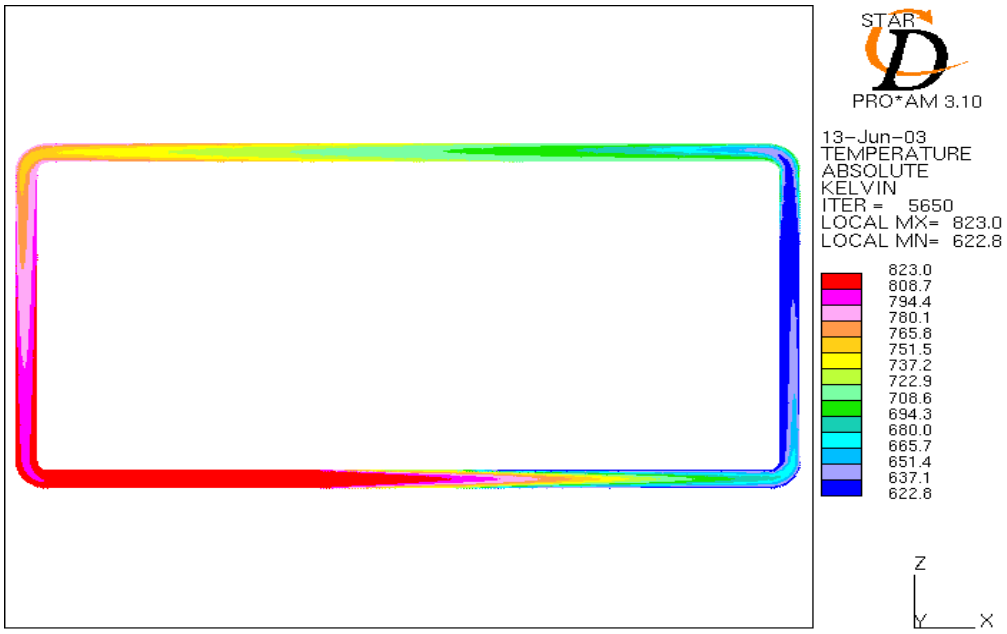

Figure 4: Temperature distribution for the laminar flow in the rectangular loop model

The diffusion in the lateral direction for laminar flow is more predominant than for the turbulent flow. This can be clearly visualized by comparing the left bottom corner elbow of figure 4 and the elbow in figure 5.

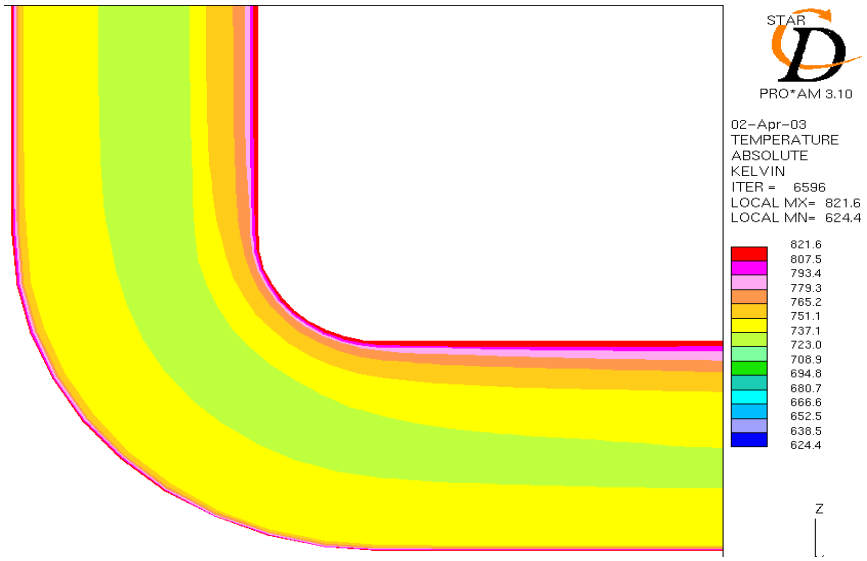

Figure 5: Temperature distribution for the turbulent flow in the rectangular loop model

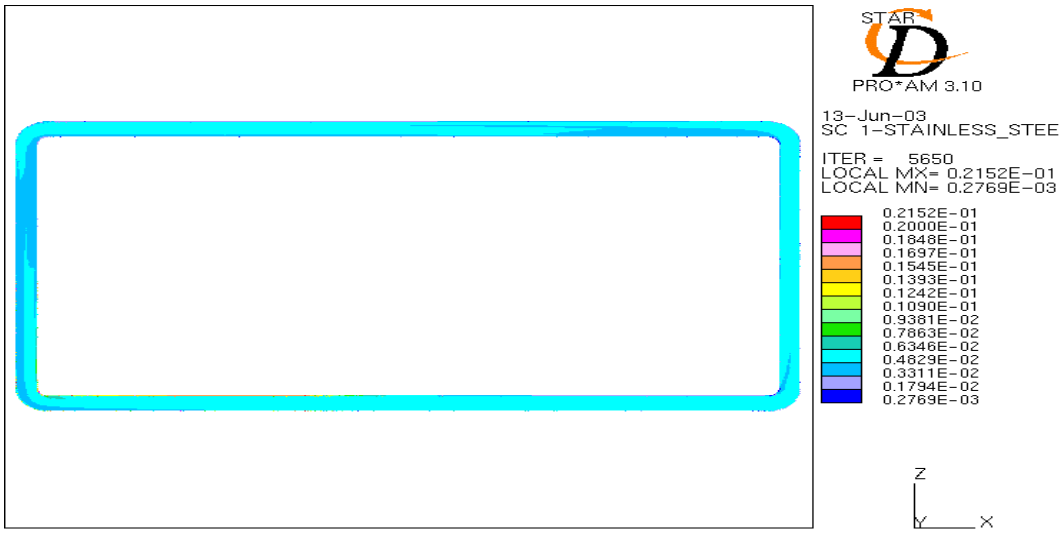

Figure 6: Concentration distribution for the laminar flow in the rectangular loop model

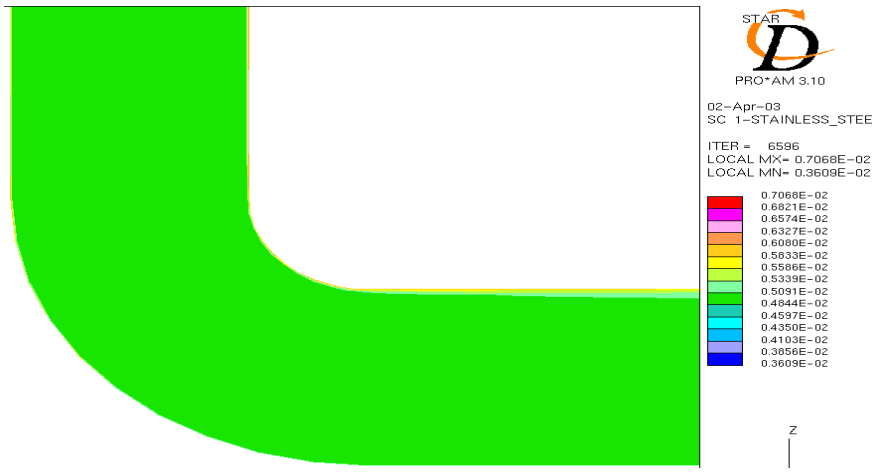

Figure 7: Concentration distribution for the laminar flow in the rectangular loop model

Figures 6 & 7 show the concentration profiles for the laminar and turbulent regimes for the rectangular loop model. The above argument for the diffusion in the lateral direction holds good for this case as well and can be envisaged as did before by comparing the two figures.

Comparison of Analytical and Simulation Models:

For the purpose of benchmarking the present package, the concentration/precipitation zones obtained from the package should be in tune with the analytical results. Hence the concentration flux, which is proportional to the concentration/precipitation rate, as explained before, has been plotted for all the three models explained above. Figure 8 shows the precipitation/corrosion rate obtained from the analytical model for an open straight pipe and a closed straight pipe models. The simulated results are being compared with the graphs corresponding to the temperature difference of 200^{o}C in fig 8.

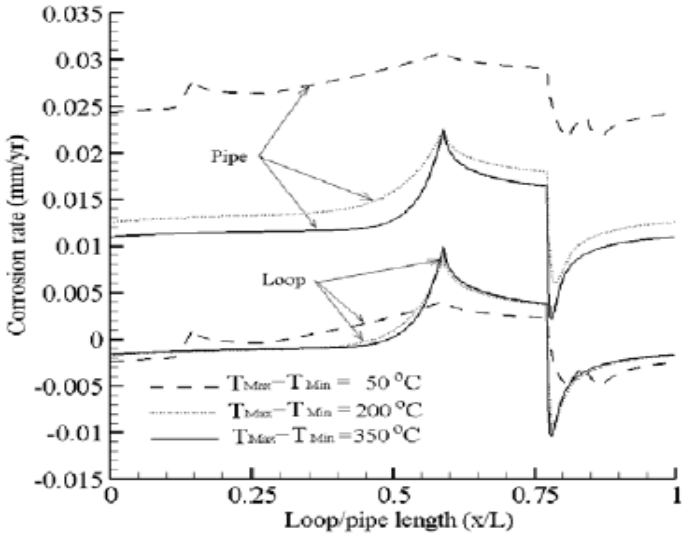

Figure 8: Corrosion/precipitation rate from the analytical models

When the regions of maximum corrosion and precipitation are compared, they fall in the same zone for both the analytical and simulated models. The reason for a larger concentration flux in the case of turbulent flow than for the laminar flow can be explained by the concept of higher lateral diffusion in the latter case. Because of the higher concentration diffusion in the laminar regime than in the turbulent regime, the concentration difference between the wall and the outermost layer of cells in the former case is lesser for the former case than the latter case

From figures 9 and 10, it can be seen that there are a few sudden falls and rises at the loop lengths, 0.15m, 0.5m, 0.65m and 1m. This trend is supposed to be because of the elbows present at those locations. Studies are still going on to find out the precise reason for this behavior. The noticeable point here is that the location of the maximum corrosion and precipitation look in good tune with the analytical results.

A grid independency check has been conducted to ensure that the results from the runs are not grid dependent. The check has been performed for both the laminar and turbulent flows. To do this test, three different grid sizes have been modeled and the results compared for all the three models. The variable of comparison used is the concentration flux along the loop length.

Figure 9 shows the grid independency check for the laminar flow and figure 10 shows the grid independency check for the turbulent flow. It can be seen that the results for all the three different grid sizes are very close to each other. For both the laminar and turbulent flows, the coarse grid refers to

39x10x1000, fine grid refers to 39x20x1000 and the finer grid refers to 39x30x1000 meshes in the ‘r’, ‘θ’ and ‘z’ directions. This confirms that the results are grid independent.

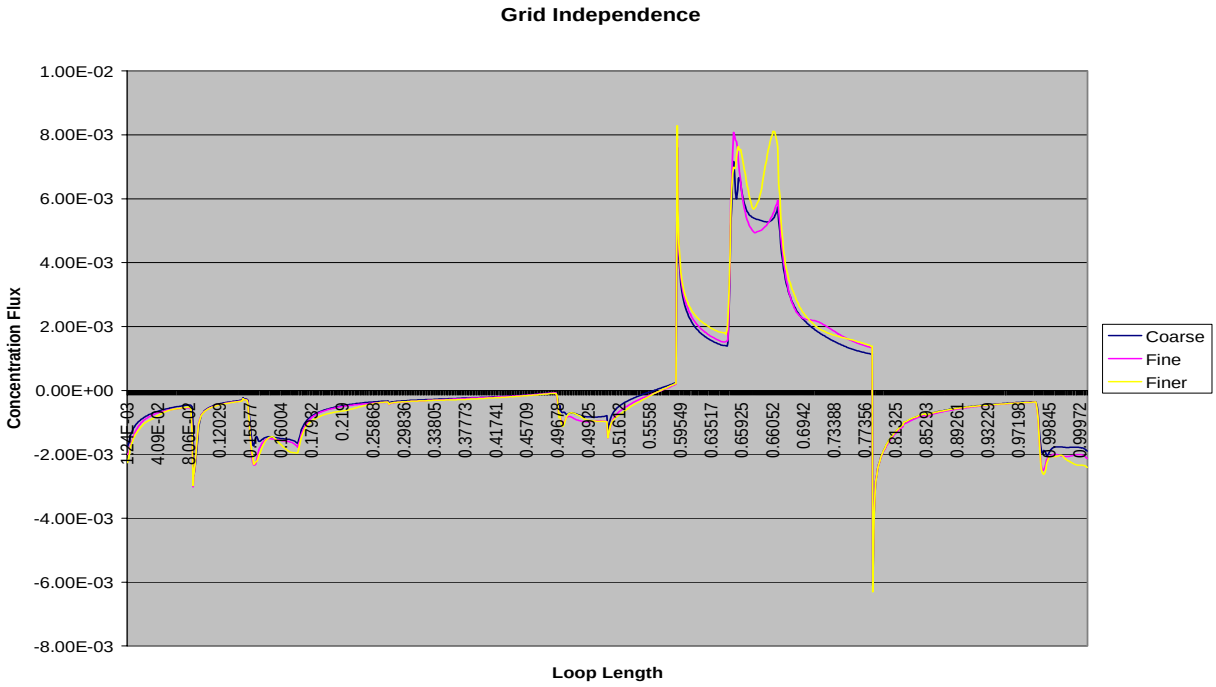

Figure 9: Corrosion/precipitation rate and grid independency check for laminar flow in a closed rectangular loop model

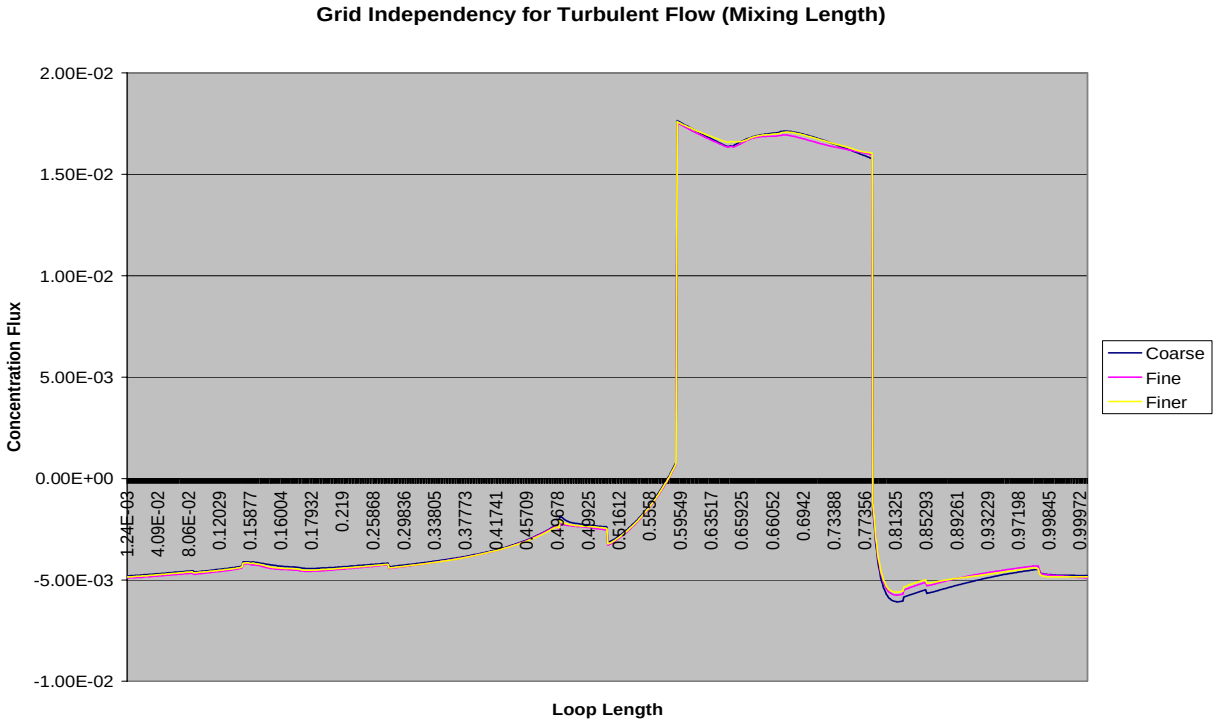

Figure 10: Corrosion/precipitation rate and grid independency check for turbulent flow in a closed rectangular loop model

Local Corrosion Modeling:

One of the important factors affecting corrosion rate is concentration gradient, especially when corrosion happens in the environment which involved complicated flow movement. Vortexes and circulations disturb the formation of boundary layer. Consequently, theoretical estimation of mass transfer phenomenon is not applicable and more uncertainties need to be considered in those kinds of situations. Flow pattern decides the way how species is washed from the wall and diffuses into bulk region. In the code, concentration gradient at wall is calculated according to expression $\frac{C_{wall} - C_{wall-1}}{\Delta y}$. In the light of unsteady nature of flow, at each cross section, concentration gradients on upper and bottom wall are taken average to show general idea of how species is transported at near-wall region along the distance to inlet.

Work is basically carried out with the parametric study of expansion ratio. Different combinations show how those factors affect species transportation. To find out the effects on mass transfer brought in by expansion ratio, three ratios were chosen to look at. They are 3, 6 and 10. Figures 11, 12 and 13 show the concentration gradients at different Reynolds Number at each expansion ratio versus distance to inlet. The results are obtained after certain amount time elapses. They are results at one instance, not averaged over time.

From those figures, we can tell that, at each expansion ratio, higher Reynolds Number generally yields higher concentration gradient. When Reynolds Number is very low, like around 10, concentration gradient varies smoothly from inlet to a certain distance and reaches its maximum value. After that point, it remains at the same value. While Reynolds Number goes up, flow becomes unsteady. Instead of smooth curve, lines start oscillating and contain numbers of peaks along X coordinate. It is because of vortexes and circulations disturb the formation of boundary layer. In near wall region, each recirculation zone affects mass transfer to a similar pattern, which is the reason why figures show several peaks with the shape close to each other. The difference between each of those oscillations in value and width is brought in by upstream which varies from one to another. One thing need to be noticed is, even though, concentration gradient lines of higher Reynolds Number in those figures seem to reach a steady situation, it is believed due to the inadequate computational time. Given more time steps, vortexes and circulations will spread to downstream along the wall.

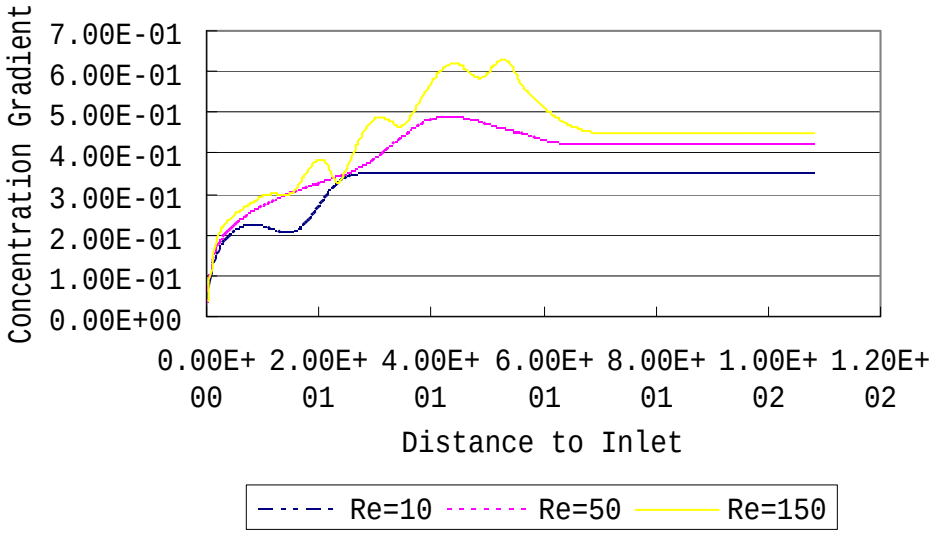

Figure 11: Concentration Gradient vs. Distance to Inlet at Expansion Ratio of 10

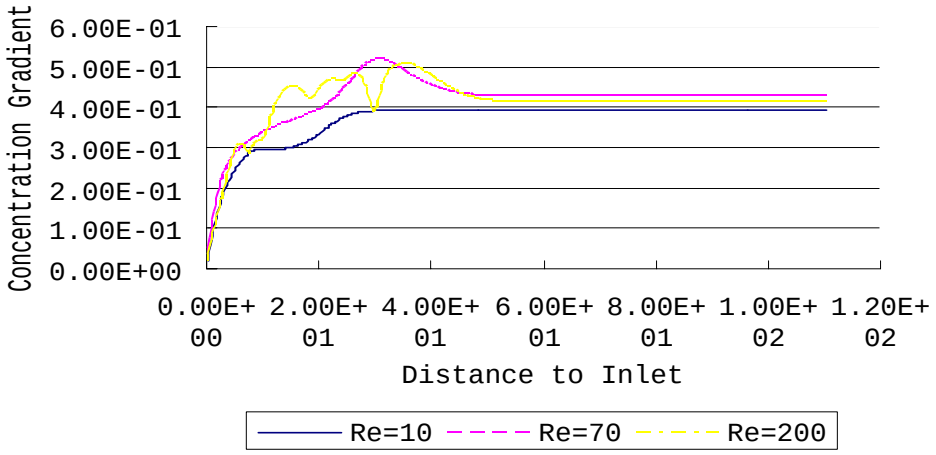

Figure 12: Concentration Gradient vs. Distance to Inlet at Expansion Ratio of 6

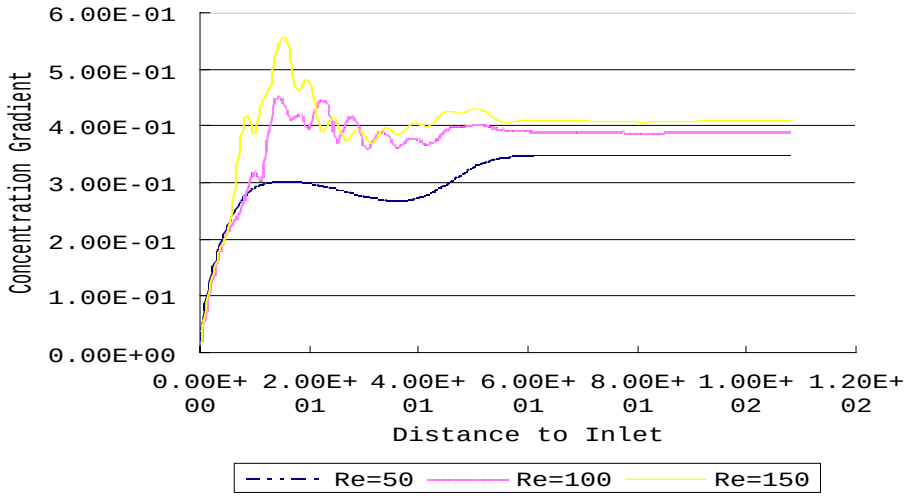

Figure 13: Concentration Gradient vs. Distance to Inlet at Expansion Ratio of 3

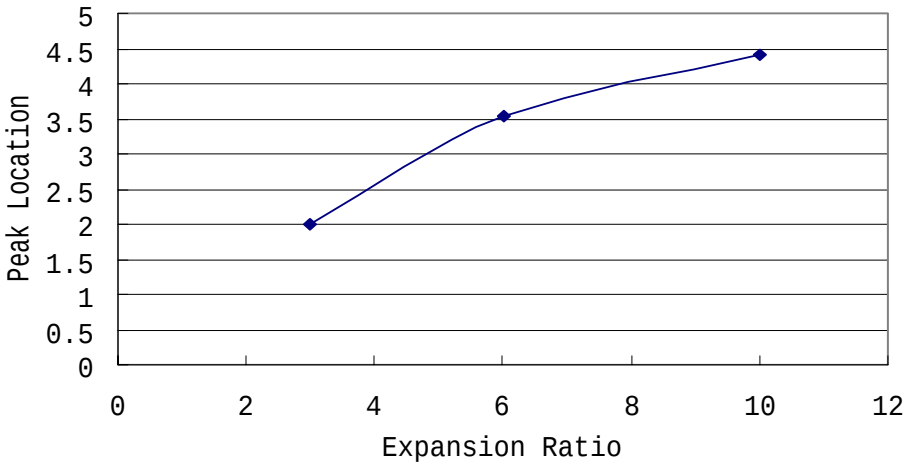

Figure 14: Peak Locations at Different Expansion Ratios

It is also can be observed that for the same expansion ratio, maximum of concentration gradient for those relatively high Reynolds Numbers occurs almost at same distance to inlet, while the value of maximum differs in the same order. With the increasing of expansion ratio, the distance to inlet where biggest concentration gradient occurs is pushed downstream. Figure 14 depicts the trend between peak location and expansion ratio.